OPEN ACCESS

Original research

Mutations in phospholipase C eta-1 (*PLCH1*) are associated with holoprosencephaly

Ichrak Drissi ,[1] Emily Fletcher,[1] Ranad Shaheen,[2] Michael Nahorski,[1] Amal M Alhashem,[3] Steve Lisgo ,[4] Alberto Fernández-Jaén ,[5] Katherine Schon,[1] Kalthoum Tlili-Graiess,[6] Sarah F Smithson,[7] Susan Lindsay,[4] Hayley J Sharpe,[8] Fowzan S Alkuraya ,[9,10] Geoff Woods [11]

► Additional material is published online only. To view, please visit the journal online (http://dx.doi.org/10.1136/jmedgenet-2020-107237).

For numbered affiliations see end of article.

Correspondence to
Dr Geoff Woods, Cambridge Institute for Medical Research Cambridge, University of Cambridge, Cambridge CB2 0XY, UK; cw347@cam.ac.uk

ID, EF and RS are joint first authors.

Received 11 June 2020
Revised 8 January 2021
Accepted 24 January 2021

To cite: Drissi I, Fletcher E, Shaheen R, *et al*. *J Med Genet* Epub ahead of print: [please include Day Month Year]. doi:10.1136/jmedgenet-2020-107237

ABSTRACT

Background Holoprosencephaly is a spectrum of developmental disorder of the embryonic forebrain in which there is failed or incomplete separation of the prosencephalon into two cerebral hemispheres. To date, dominant mutations in sonic hedgehog (SHH) pathway genes are the predominant Mendelian causes, and have marked interfamilial and intrafamilial phenotypical variabilities.

Methods We describe two families in which offspring had holoprosencephaly spectrum and homozygous predicted-deleterious variants in phospholipase C eta-1 (*PLCH1*). Immunocytochemistry was used to examine the expression pattern of PLCH1 in human embryos. We used SHH as a marker of developmental stage and of early embryonic anatomy.

Results In the first family, two siblings had congenital hydrocephalus, significant developmental delay and a monoventricle or fused thalami with a homozygous *PLCH1* c.2065C>T, p.(Arg689*) variant. In the second family, two siblings had alobar holoprosencephaly and cyclopia with a homozygous *PLCH1* c.4235delA, p.(Cys1079ValfsTer16) variant. All parents were healthy carriers, with no holoprosencephaly spectrum features. We found that the subcellular localisation of PLCH1 is cytoplasmic, but the p.(Cys1079ValfsTer16) variant was predominantly nuclear. Human embryo immunohistochemistry showed PLCH1 to be expressed in the notorcord, developing spinal cord (in a ventral to dorsal gradient), dorsal root ganglia, cerebellum and dermatomyosome, all tissues producing or responding to SHH. Furthermore, the embryonic subcellular localisation of PLCH1 was exclusively cytoplasmic, supporting protein mislocalisation contributing to the pathogenicity of the p.(Cys1079ValfsTer16) variant.

Conclusion Our data support the contention that PLCH1 has a role in prenatal mammalian neurodevelopment, and deleterious variants cause a clinically variable holoprosencephaly spectrum phenotype.

INTRODUCTION

Holoprosencephaly is a structural anomaly of the brain in which there is failed or incomplete separation of the embryonic prosencephalon into two cerebral hemispheres and associated bilateral structures. In humans, the defect causing holoprosencephaly arises between the third-week and fifth-week postfertilisation.[1] The most severe forms of holoprosencephaly are classified as alobar, semilobar and lobar, and the greater the degree of holoprosencephaly, the greater the degree of intellectual deficit and associated congenital anomalies.[2] These include facial anomalies (ranging from cyclopia and a proboscis to a single upper incisor, to none), central (and bilateral) cleft lip and palate, congenital heart disease, preaxial polydactyly and endocrine deficiencies.[2 3]

The prevalence of holoprosencephaly is estimated to be 1/250 in conceptuses and 1/16 000 live births.[4] The aetiology of human holoprosencephaly is varied: environmental (eg, maternal diabetes gives a 1% risk to the fetus), chromosomal (the most common overall cause, an example being trisomy 13), Mendelian or unknown.[2] Mendelian causes are subclassified into non-syndromic (which are inherited as dominant disorders) and syndromic (where there are additional distinctive features, and inheritance can be either dominant or recessive).[2] Many of the 14 genes known to cause holoprosencephaly are involved in the sonic hedgehog (SHH) signalling pathway.[5 6]

The study of families with genetic form of holoprosencephaly extended the spectrum of brain and facial anomalies to include the milder phenotypes. The 'middle interhemispheric fusion variant' consists of syntelencephaly (where posterior, frontal and parietal areas lack midline separation and/or lack of cleavage of the basal ganglia and thalami, and absence of the body of the corpus callosum). 'Microform holoprosencephaly' is a much milder form where the brain is structurally normal, but there are subtle craniofacial anomalies with or without mild neurocognitive impairment.[7–9]

A marked variability of phenotype is a constant finding in the Mendelian disorders associated with holoprosencephaly, and this variability is seen within families, and between individuals in different families with the same mutation.[2 10] The degree of phenotypical variability seen in dominant disorders that cause holoprosencephaly is unusually marked, and this variability is also seen in the recessive disorder Smith-Lemli-Opitz syndrome (SLOs), where consistency of phenotype may have been expected.[11] The causes of this variability are unknown but are considered related to three factors: the complexity of the developmental

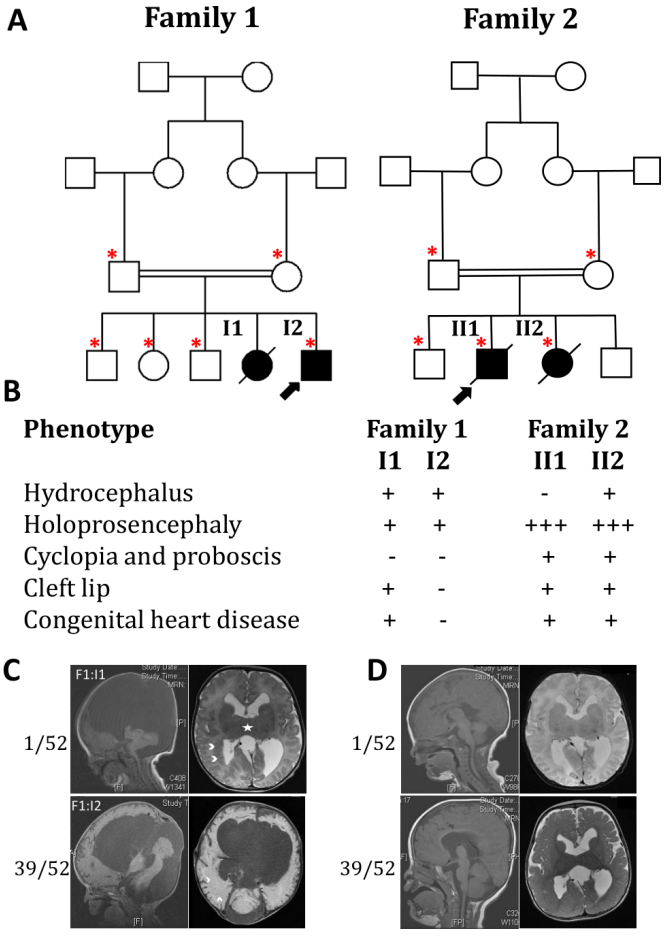

Figure 1 Family pedigrees, summary phenotype table and brain scans of affected individuals. (A) Pedigrees of the two families described in the paper. Arrows show probands; filled-in squares or circles denote affected individuals; and red asterisks denotes people from whom we had a DNA sample. (B) Key phenotypical features of the affected four children aligned; all other family members have no disease features. A minus sign designates the feature was absent; a plus sign indicates it was present; and a triple plus sign indicates that the features were severe. (C,D) MRI brain scans of the two affected children from family 1, detailed in the text. For each, the top pair of scans shows results for 1 week of age, and the lower pairs for 39 weeks of age. (C) Gross hydrocephalus and the later findings were suggestive of holoprosencephaly. In both right-hand axial T2 views, the star shows the fused thalami, and two ventricular heteropias are best seen in the upper axial T2 view shown by arrow heads. (D) Lesser hydrocephalus with partial thalamic fusion, again a feature of the holoprosencephaly spectrum.

pathways in which SHH participates (in consort with transforming growth factor-β (TGF-β) and fibroblast growth factor (FGF) pathway signalling); that otherwise harmless polymorphisms in holoprosencephaly-related genes could become disease modifiers; and that the environmental/maternal factors such as alcohol, diabetes and cholesterol intake and metabolism can affect the intracellular and intercellular environments resulting in altered SHH signalling.[12–14]

We document two families in which children have severe developmental delay secondary to brain malformations within the holoprosencephaly spectrum. We were unable to find any known cause of their phenotypes but did discover homozygous, very rare, predicted deleterious variants in the phospholipase C eta-1 (*PLCH1*) gene. Our clinical and molecular results suggest that biallelic mutations in *PLCH1* are a novel cause of holoprosencephaly.

METHODS

Clinical studies

The authors ascertained families by direct referral from the family's paediatricians or clinical geneticists. The family details and pedigrees were recorded by their physicians, informed consent obtained for diagnostic genetic studies and blood samples taken for DNA extraction. All clinical observations, studies and tests were performed to enable a diagnosis and guide treatment; none was performed solely for research purposes. Families and their physicians were informed of the research findings.

Molecular genetic analysis seeking pathogenic variants

The two families were separately ascertained and clinically investigated. No further families were notified to us after a GeneMatcher request; gnomAD shows no homozygous loss of function variants; and there were no cases reported in the DECIPHER study.

In each family, the affected individuals' genomic DNA was extracted from blood samples by standard methods—in family 1, DNA was only available from the affected son and unaffected parents; in family 2, DNA was available from both affected cases and their unaffected parents. Exome analysis was performed on the affected individual's DNA (SureSelect Human All Exon 50 Mb Kit, Agilent Technologies). Potentially pathogenic mutations were identified by comparison with the GRCh37 reference human genome, filtering for changes with allele frequencies of <1 in 500 in the ExAC database (now incorporated within the genomAD database), and focused on homozygous and biallelic changes (and concordance between siblings in family 2). Novel unreported variants and known single-nucleotide polymorphisms (SNPs) were then sought that could be pathogenic by SIFT (missense variants) or by filtering (lost start and stop codons, premature nonsense variants, small insertions and deletions, and canonical splicing variants) in the exome results of the affected individuals of each family. A summary of the filtering process to discover potentially pathogenic variants in the two families is given in online supplemental table 1). Separately, all variants and SNPs in known holoprosencephaly genes were reviewed by hand. Any potential pathogenic variants were confirmed and tested for expected recessive segregation by PCR and Sanger sequencing of the parents and their affected offspring.

Microarray analysis seeking chromosome perturbations was performed in all four affected individuals. PLCH1 has three isoforms reported. We used the most common and longest transcript for our studies NM_001130960, which contains both of the mutations we report.

Re-examination of family genetic data seeking changes in holoprosencephaly-related genes

The following genes implicated are in SHH signalling and holoprosencephaly: *BOC*, *CDON*, *DISP1*, *DHCR7*, *DLL1*, *FGF8*, *FOXH1*, *GAS1*, *GLI2*, *NODAL*, *PTCH1*, *SHH*, *SIX3*, *TDGF1*, *TGIF1*, *SUFU* and *ZIC2*. All exons were adequately covered in our exome analysis for base changes and small INDELS.[15] For these genes, we sought both novel variants and known SNPs that would be predicted as potentially pathogenic in the exomes of each family's affected individuals. To find exon/gene scale deletions and duplications in these genes, we both re-examined microarray analyses of the affected children and examined

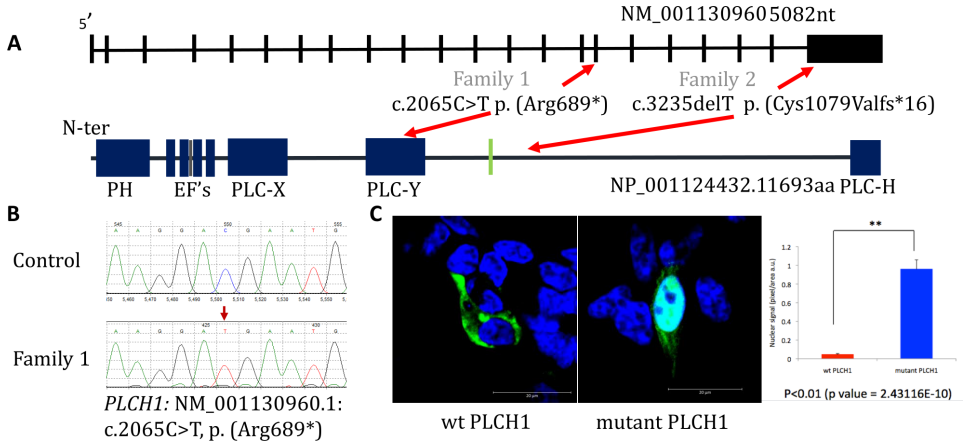

Figure 2 PLCH1 gene and protein, with position of mutations, and subcellular localisation of PLCH1 wild type and family 2 mutation p.(Cys1079ValfsTer16). (A) Uppermost is a cartoon of the structure of the *PLCH1* gene. The relative size of the exons, but not introns, is shown. Lowermost is a cartoon of the PLCH1 protein with the canonical PLCH domains in blue and named, a predicted nuclear localisation signal is shown in black, and predicted nuclear export signal in green. Between the gene and the protein, the family 1 and family 2 mutations are shown, with their respective postions in gene and protein indicated. (B) Electrophoretogram of the family 1 mutation, with upper homozygous wild-type control and lower homozygous mutation. (C) Subcellular localisation of wild-type PLCH1 on the left to be cytoplasmic in a transfected 1-7HB2 epithelial cell line, whereas the middle pane shows that the family two mutation P. (Cys1079Valfs*16) is also present in the nucleus. on the right a bar chart shows the nuclear signal depicted by pixel/area of PLCH1 covered in the nucleus of WT PLCH1 (red) and mutant PLCH1 (blue). A two tailed t-test performed on the data gave a p value of 2.43116E-10, so p<0.01 and the mutant and WT PLCH1 nuclear signals are significantly different p<0.01, so mutant PLCH1 shows a statistically significant increase in nuclear signal. Methodology if needed for subcellular localisation of mut v wt: cellular localisation of the WT PLCH1 protein and mutant PLCH1 protein, showing a clear change in localisation to include in the nucleus in 1-7HB2 epithelial cell line, with PLCH1 being stained with antiFLAG (goat anti-rabbit 488) in green at 1:1000 and DAPI nuclear staining in blue. These were viewed using confocal microscopy at ×100. PLCH1, phospholipase C eta-1.

sequencing depth by comparative analysis of affected versus controls in the Integrated Genome Viewer.

Gene cloning, tagging and mutagenesis of PLCH1

The plasmid pFLAG-CMV2 wild-type *PLCH1* was manufactured from IMAGE clone IRATp970F03110D (Source BioScience) of *PLCH1* isoform NM_001130960, generating pFLAG-PLCH1. The p.Cys1079ValfsTer16 variant was introduced into pFLAG-PLCH1 using the QuikChange mutagenesis (Stratagene, USA) protocol, using the following primers: (forward) 5′CAGGAAAA CCCCTTCCCAGCAAGTC and (reverse) 5′GACTTGCTGGGA AGGGGTTTTCCTG.

Subcellular localisation studies of PLCH1 and PLCH1 p.(Cys1079ValfsTer16)

HEK 293 cells were grown in Dulbecco's modified Eagle's medium (Invitrogen), supplemented with 10% fetal calf serum, 1% L-glutamine and 1% non-essential amino acids (Invitrogen). Cells were grown in a 95% air, 5% CO_2 atmosphere at 37°C. Prior to transfection cells were plated to 60%–70% confluency on Poly-D-Lysine coated glass coverslips and transfected using Fugene HD (Promega) for 24 hours with four µg of pFLAG-PLCH1. All incubations were performed at room temperature and cells were analysed 72 hours post-transfection. Transfected cells were washed with PBS before and after a 10 min fixation with 4% paraformaldehyde and blocked in 10% donkey serum and 10% immunohistochemistry (IHC) blocking buffer (Sigma) diluted in PBS 0.1% Triton buffer (PBS-T) for 30 min. To detect PLCH1 variants tagged with FLAG, cells were incubated with rabbit anti-FLAG antibodies (Sigma) diluted 1:100 in PBS-T supplemented with 10% donkey serum for 2 hours. Cells were washed three times in PBS-T for 10 min before protein labelling with donkey anti- rabbit 488 antibodies (Invitrogen) diluted 1:1000 in PBS-T for 45 min. Coverslips were washed before mounting using Fluromount-G DAPI (Invitrogen), and cells were viewed using the Zeiss LSM780 confocal microscope system.

IHC of PLCH1 expression in human embryos

The CS10, CS12 and CS13 human embryonic sections were provided by the Human Developmental Biology Resource, which is regulated by the Human Tissue Authority and operates in accordance with the relevant codes of practice. Embryos were collected from women undergoing social termination of pregnancy with appropriate maternal written consent and approval from the Newcastle and North Tyneside NHS Health Authority Joint Ethics Committee. The samples were staged using the guidelines of Bullen and Willson, fixed in methacarn (60% absolute methanol, 30% chloroform and 10% glacial acetic acid) and processed through to paraffin wax (fibrowax, VWR).[16] Sections were taken on a microtome at 7 μm thickness and mounted on Superfrost Plus microscope slides (Thermo Scientific).

Sections were dewaxed with Histo-Clear (National Diagnostics), rehydrated in graded ethanol and rinsed in distilled water. Antigen retrieval was performed by heating the sections to 95°C in sodium citrate buffer pH 6 for 20 min. Cooled sections were rinsed in distilled water before 2 and 5 min permeabilisation washes in Tris–HCL 0.1% Triton buffer pH 10 (Tris–HCL–T buffer). To prevent non-specific staining, sections were blocked in 10% donkey serum and 10% IHC blocking buffer (Sigma) diluted in Tris–HCL–T buffer for 90 min. Sections were incubated overnight at 4°C in a humidified chamber with rat polyclonal anti-SHH antibody (Abcam, ab50515) and rabbit polyclonal anti-human PLCH1 (Genetex, GTX108612), both diluted 1:100 in Tris–HCL–T buffer containing 10% donkey serum. After washing with Tris–HCL–T buffer, sections were labelled for 2 hours at room temperature with donkey anti-rabbit IgG-488 (Invitrogen) and donkey anti-rat IgG-546 (Invitrogen). Slides were washed with Tris–HCL buffer and mounted using

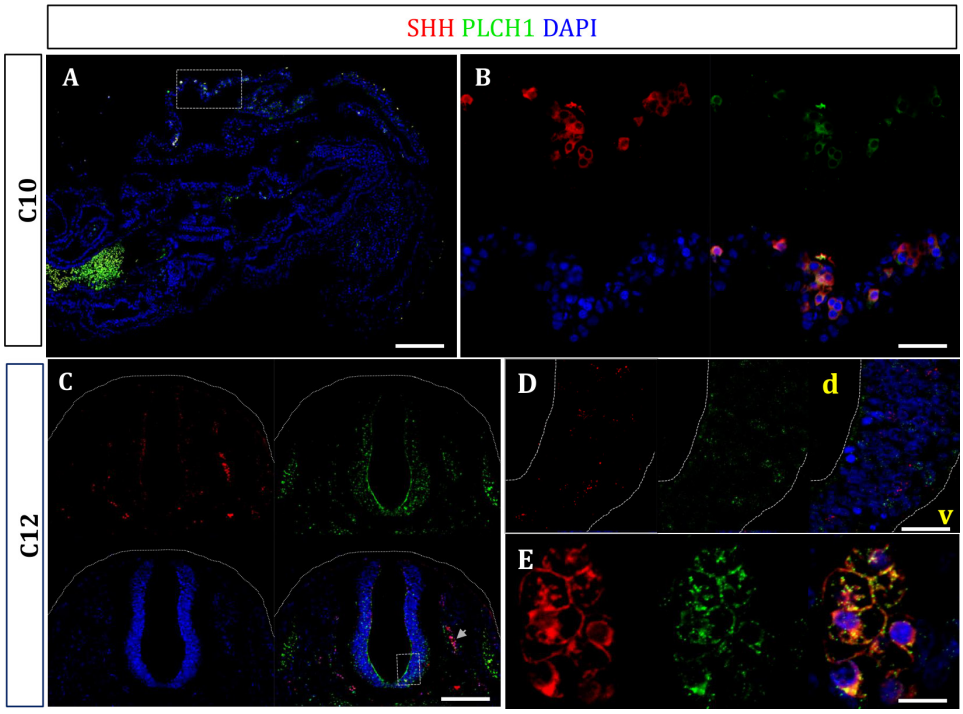

Figure 3 Human embryo immunohistochemistry studies expression of PLCH1 and SHH in a carnegie stage 10 sagittal section and carnegie stage 12 transverse section through the upper thorax. Antibodies to human SHH are shown in red; antibodies to PLCH1 are shown in green; and DAPI in blue shows nuclei. (A) Near midline sagittal section of a CS10 embryo, with size bar 100 µm. The boxed area contains cells with both SHH and PLCH1 expression and is shown magnified in B. The green mass to the lower left is artefact autofluorescence. The orientation of the embryo is unclear, but probably the head is at the right top with the back at the bottom and abdominal area to the left side. (B) Magnification of the boxed area in A, size bar 40 µm. The upper left panel is of SHH expression, upper right of PLCH1, lower left of DAPI and the composite is at the lower right and shows a collection of cells, most of which express both SHH and PLCH1. (C) Transverse CS12 section through the upper thorax, with size bars 100 µm. The upper left panel is of SHH expression, upper right of PLCH1, lower left of DAPI and the composite is at the lower right showing the spinal cord at the centre including a boxed area, developing dorsal root ganglia at either side—on the right indicated by an arrow and laterally the somites stained prominently by PLCH1. (D) Magnification of the boxed area in C, size bar 25 µm. the left panel is of SHH expression, middle of PLCH1, and the composite is at the right also including DAPI. It shows that some cells in the developing spinal cord express SHH or PLCH1, but rarely both. (E) Magnification of the arrowed area in C, size bar 10 µm. The left panel is of SHH expression, middle of PLCH1, and the composite is at the right also including DAPI. This shows that the cells of the developing dorsal root ganglia predominantly express both SHH and PLCH1. PLCH1, phospholipase C eta-1; SHH, sonic hedgehog.

Fluromount-G DAPI (Invitrogen). Specimens were visualised using the Zeiss LSM780 confocal microscope system.

RESULTS

Clinical findings in the two families

Inheritance pattern: in each family there were both affected and unaffected children; the parents were unaffected (no features of the holoprosencephaly spectrum or other congenital anomalies or intellectual or neurological deficit); affected children were of both sex; parents were consanguineous (see figure 1A). There were no known affected individuals in the wider pedigrees. From this we concluded that the most likely inheritance pattern of the phenotypes in both families was autosomal recessive.

Full clinical phenotype details are given in the online supplemental file and summarised here and in figure 1B–D. In family 1, the parents were Saudi first cousins and had three normal children. A 5-year-old boy, and in retrospect his deceased sister, were both affected and born with macrocephaly secondary to hydrocephalus. In the girl, postnatal brain MRI revealed a large posterior fossa cyst with atrophy of the cerebellum and partial agenesis of the vermis, heterotopias in both cerebral hemispheres, posteriorly kinked midbrain, atrophic pons, and a disfigured ventricular system giving the appearance of a mono-ventricle with absent septum pellucidum. The later findings were suggestive of holoprosencephaly (see figure 1C). In the boy, a postnatal brain MRI at 1 week revealed a subependymal cyst near the foramen of Monro and partial agenesis of the corpus callosum. Repeat MRI at age 9 months showed partial thalamic fusion, evolving cerebral leucomalacia and apparent aqueduct stenosis (see figure 1D). Both children developed tonic–clonic epilepsy postoperatively and had gross motor and cognitive delay evident by 2 years. The girl also had a ventricular septal defect, cleft lip and palate (bilateral cleft lip and palate). In summary, both children had complex brain anomalies within the holoprosencephaly spectrum.

in family 2, the parents were Pakistani first cousins with two normal children. Their first affected child was a male infant who had alobar holoprosencephaly detected by antenatal ultrasound at 20 weeks of gestation. He was born at term but died shortly after birth. He was confirmed to have alobar holoprosencephaly and also cyclopia, a midline cleft lip, microcephaly (−3 SD) and cardiac anomalies (double outlet right ventricle, ventricular septal defect and possible aortic atresia). The parents declined postmortem examination. A second pregnancy, a woman, also had holoprosencephaly, with gross hydrocephalus. She also died a few hours after birth. She had no eyes but disrupted tissue beneath a proboscis, and her ears were joined together under her chin. The parents declined postmortem examination. In

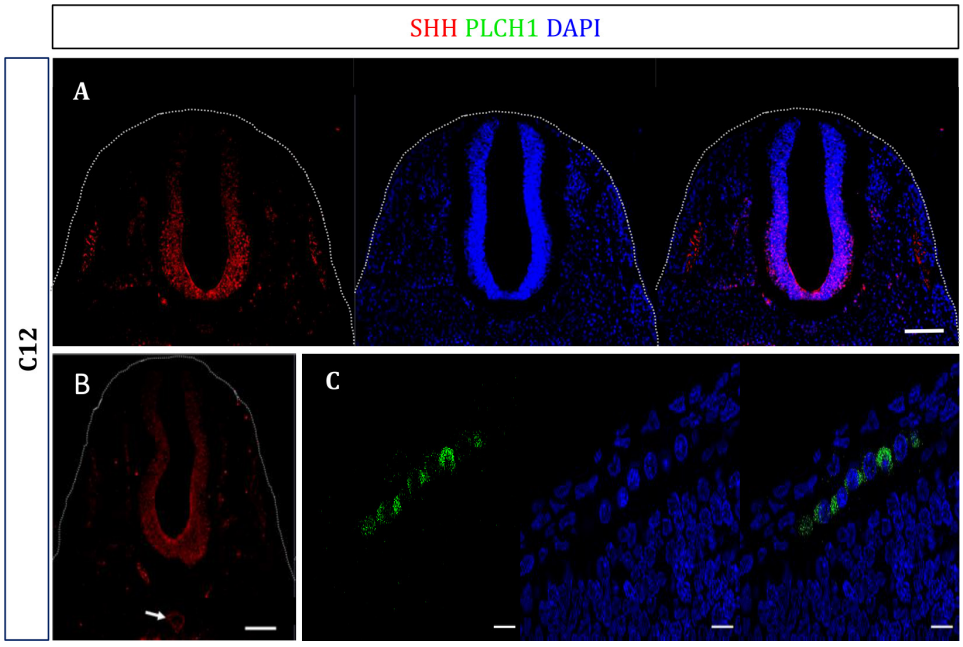

Figure 4 Human embryo immunohistochemistry studies in carnegie stage 12 transverse sections illustrating a PLCH1 ventrodorsal gradient in the spinal cord, notocord expression and that embryonic subcellular localisation of PLCH1 is consistently cytoplasmic and not nuclear. Antibodies to human PLCH1 are shown in red, and DAPI in blue shows nuclei. (A) Transverse CS12 section through the upper thorax, with size bars 100 µm. Leftmost is PLCH1 expression; middle DAPI and the composite at right. This shows the ventrodorsal gradient of PLCH1 expression in the developing spinal cord – mirroring a similar reported SHH gradient. The laterally placed somites also express PLCH1. The dorsal root ganglia (between the somites and spinal cord) also express PLCH1 but are less well shown. This is likely a consequence of the somites and spinal cord being continuous, but the dorsal root ganglia being an intermittent chain of cell aggregates. (B) Transverse CS12 section through the upper thorax, with size bars 100 µm; only staining for PLCH1 expression is shown. the white arrow shows PLCH1 expression in the notochord; the ventrodorsal gradient of PLCH1 expression in the developing spinal cord is again shown. (C) Sagittal C12 section with size bar 10 µm. Leftmost is PLCH1 expression, middle DAPI and the merge at right. This shows a cytoplasmic subcellular localisation of PLCH1 in the hindbrain. PLCH1, phospholipase C eta-1; SHH, sonic hedgehog.

summary, the babies both had a severe holoprosencephaly phenotype, and their diagnosis would include Young-Madders syndrome, SLOs or any of the single gene causes of holoprosencephaly sequence—although the absence of polydactyly in both affected babies would be uncommon.[17]

Molecular genetic analysis seeking pathogenic variants

In both families, we analysed the exome data assuming a recessive mode of inheritance, seeking both biallelic and homozygous pathogenic variants, and that were concordant between the affected individuals in family 2. No potential mutations were found in any known holoprosencephaly gene. There were no potential biallelic mutations in either family. Microarray analysis of affected individuals were normal.

Figure 2A shows *PLCH1*, the PLCH1 protein, and the variants found in each family. In family 1, we found a homozygous nonsense variant in the affected son, c.2065C>T in *PLCH1*, which leads to a premature stop codon p.(Arg689*) in exon 16 (of 22 exons) and hence likely subject to nonsense mediated mRNA decay (see figure 2B). In family 2, a homozygous one base deletion in *PLCH1* c. 3235delT was found, predicted to result in p.(Cys1079ValfsTer16). The deletion was in the last exon on *PLCH1* and so would not be expected to be subject to nonsense mediated mRNA decay, but instead to yield a truncated protein with the C-terminal 623 amino acids (of 1693) deleted. Both of these mutations were confirmed as real, and to segregate as expected for a recessive genotype within families.

These *PLCH1* variants have not been previously reported and are absent from gNOMAD.

Re-examination of family genetic data seeking changes in holoprosencephaly and SHH-related genes

In family 1 and family 2, we found no potential pathogenic variants in known SHH or holoprosencephaly-related genes. In family 1, PLCH1 variant was the only high-quality novel homozygous coding variant with deleterious prediction identified within the autozygome of the index. In family 2, the following protein altering SNP genotypes were present in both affected babies: in DISP1 heterozygous rs2609383 p.(Glu103Lys) with global minor allele frequency (GMAF)=0.1814, and heterozygous rs2789975 p.(Glu103Asp) with GMAF=0.1819; in NODAL homozygous rs1904589 p.(His165Arg) with GMAF=0.343; in CDON homozygous rs3740912 p.(Val75Ile) with GMAF=0.4525, heterozygous rs3740909 p.(Glu162Lys) with GMAF=0.1074 and homozygous rs684535 p.(Ile1221As) with GMAF=0.2002. In PTCH1 rs357564 p.(Pro1315Leu) with GMAF=0.390 was homozygous in one and heterozygous in the other. None of these SNPs is reported to have functional effects.

Subcellular localisation studies of PLCH1 and the PLCH1 mutation p.(Cys1079ValfsTer16)

We found that wild-type PLCH1 was localised solely to the cytoplasm (see figure 2C). We had expected a nuclear localisation as a bipartite nuclear localisation motif was predicted to be present in PLCH1 (see figure 2A). The localisation of the mutant p.(Cys1079ValfsTer16) PLCH1 was either nuclear and cytoplasmic (25%), or only nuclear (75%) (see figure 2C). Therefore,

Table 1 Comparison of the incidence of phenotype features of selected conditions in which holoprosencephaly is common from literature review*

	Our cases†	Smith-Lemli-Opitz syndrome	Young-Madders syndrome	Trisomy 13	SHH mutation phenotype
Mode of inheritance	Recessive	Recessive	Recessive	Sporadic dominant	Autosomal dominant
Holoprosencephaly (%)	4/4	5	100‡	30	36
Characteristic facies (%)	>90	>90	>90	60	>60
Cleft lip (%)	3/4	40	53	40	20
Congenital heart disease (%)	3/4	50	15	80	2
Microcephaly (%)	1/4	80%	12	20	10
Male ambiguous genitalia (%)	0/2	50	60	0	5
Intellectual deficit range (%)	4/4 severe	Normal (>5%) to severe	100% severe	100% severe	Normal (30%) to severe
Postaxial polydactyly (%)	0/4	33	90‡	80	<10
2/3 toe syndactyly (%)	0/4	>90	10§	0§	0§

*From the references in the text.
†As we describe four cases, we give numbers not a percentage.
‡Presumably a bias introduced by the disease definition.
§Presumably under-reported.
SHH, sonic hedgehog.

the pathogenic mechanism of the p.(Cys1079ValfsTer16) may be both of loss of the C-terminal domain, and also reduced protein availability at its site of action within critical cells. Furthermore, these results suggest the possibility that the PLCH1 nuclear localisation signal can be functional, and that the C-terminus of PLCH1 is able to block/mask this motif, potentially enabling the protein to change subcellular localisation. We found no evidence of PLCH1 expression in primary cilia using overexpression studies, in accord with published proteomics experiments (see online supplemental figure 1).[18]

Determination of the human embryonic expression pattern of PLCH1

Holoprosencephaly and the other developmental structural brain anomalies seen within the holoprosencephaly spectrum brain are thought to arise between human embryonic week 3 and embryonic week 5. This commences with human embryonic Carnegie stage 8, when the human midline notochord induces changes in the prechordal plate, which is anterior and lateral to the notochord (the prechordal plate is destined to become the prosencephalon, ultimately giving rise to all forebrain structures). By embryonic week 5, Carnegie stage 15, the prosencephalic structures, including the thalami, have formed, become distinct and separated.[1] We did not attempt to perform a complete study of this developmental period, as the necessary embryo sections are unavailable.

The earliest embryo we were able to obtain was approximately Carnegie stage 10. SHH and PLCH1 both colocalise to the same small region of the embryo; both have a cytoplasmic subcellular localisation, but embryonic anatomical structures were impossible to accurately define (see figure 3A,B).

Thereafter, the earliest embryo sections available were of Carnegie stage 12. We chose to examine a transverse sectioned Carnegie stage 12 embryo, a time-point when the spinal cord neural precursors are developing into different neuronal classes dependent on a dorsal bone morphogenic protein (BMP) gradient and a counter ventral SHH gradient. As expected, SHH is expressed in the spinal cord, acting as a control for the embryo age and anatomy (see figure 3C,D). We found PLCH1 was also expressed with a clear ventral–dorsal gradient (greatest nearest the notochord; see figures 3C,D and 4A). Both SHH and PLCH1 are coexpressed in the developing dorsal root ganglia (identified by neutrophic tyrosine kinase receptor type 1 (TRKA) expression, results not shown; see figure 3E). PLCH1, but not SHH (as expected[19]), is expressed in the laterally placed somites, (see figures 3C and 4A). We also found SHH and PLCH1 present together in the notochord in transverse sectioned Carnegie stage 12 embryo (figure 4B). Consistently, PLCH1 had a cytoplasmic subcellular localisation and is not seen in the nucleus, as best shown in the hindbrain in sagittal sectioned Carnegie stage 12 embryo in figure 4C. The sections in figure 3 and figure 4A–C are each from different embryos.

These results show considerable colocalisation of PLCH1 with SHH in the human embryonic nervous system. The results suggest that PLCH1 has more than one role in human embryonic development. The gradient of PLCH1 in the developing spinal cord is compatible with a role in neural precursor/early neurons being able to respond to SHH (as does the presence of PLCH1 alone in somites). However, the presence of PLCH1 in the notochord supports a role in SHH secretion.

DISCUSSION

We describe two families with a holoprosencephaly phenotype, one with extreme alobar holoprosencephaly and expected facial and cardiac malformations, the second with malformations restricted to the central nervous system (CNS). However, marked variability is common and expected in both dominant and recessive Mendelian diseases causing holoprosencephaly, and for this reason, we pursued the finding of homozygous variants in *PLCH1* as being a possible novel Mendelian cause of the holoprosencephaly spectrum in these families.[2 10 11]

We first compared our cases to those of the best known recessive diseases in which holoprosencephaly is a feature, SLOs and Young Madders syndrome (also known as pseudo-trisomy 13 syndrome), sporadic Trisomy 13 and the dominant SHH mutation phenotype[20] (see table 1). Our cases are similar to those with Young-Madders syndrome and trisomy 13, but do exhibit the phenotypical variability seen in recessive SLOs and dominant SHH mutations. Severely affected SLOs individuals have only a few possible differences to our cases, the presence of 2/3 toe syndactyly, ambiguous genitalia, and polydactyly—all of which are extra-CNS anomalies.[11] Young-Madders syndrome has the same phenotype as trisomy 13, with the karyotype distinguishing between the two.[17 21] The gene causing Young-Madders syndrome has not been discovered (probably resulting in underascertainment of more milder affected cases), although the only report of a consanguineous child in which homozygosity mapping was performed revealed 21 regions of homozygosity—one of which included *PLCH1*[22] (an a priori 10% chance[23]), so *PLCH1* could be the cause of Young-Madders syndrome. The genes responsible for trisomy 13 phenotype are unclear, but polyalanine expansions, deletions and a duplication of ZIC2 (on chromosome 13)

have been reported in cases of holoprosencephaly without other known causes.[24]

The developmental processes that are considered to go awry in human holoprosencephaly occur between weeks 3 and 6 postfertilisation. We therefore asked if there was evidence that PLCH1 was expressed in the human embryo during this period. While PLCH1 was considered to be expressed exclusively in the CNS, there were no expression data available for this early period in human or murine embryos, and so we generated this.[25 26] We used SHH as a marker of developmental stage and of early embryonic anatomy, and to see if PLCH1 and SHH were ever co-expressed. Results for a fourth-week embryo were limited to showing coincidence of expression of cytoplasmic PLCH1 and SHH in a contiguous region of cells, but we were unable to define the anatomy of the section. In fifth-week human embryo transverse sections of the upper thorax, we found that PLCH1 and SHH were both expressed in the developing spinal cord, the notochord and dorsal root ganglia. PLCH1 exhibited a ventral–dorsal gradient in the spinal cord, mimicking the known SHH morphogenic gradient, and the opposite of that of BMPs and WNTs. PLCH1 alone was detected in somites, which do not express SHH but respond SHH produced in the spinal cord. This data set is incomplete and, most importantly, we were not able to assess PLCH1 expression in the precordal plate (beginning of third week postfertilisation) as human embryonic samples were not available. However, we have shown SHH expression to be anatomically and developmentally as expected in the fifth week postfertilisation (as shown in our Carnegie stage 12 and 13 results), and that PLCH1 and SHH have coincident expression in all neural tissues.

How could PLCH1 deficiency cause holoprosencephaly? Phospholipase C Eta-1 and Eta-2 (genes *PLCH1* and *PLCH2*) are members of the most recently discovered class of the phospholipase C family.[27] As with all members of the phospholipase C family, on activation, PLCH1 increases intracellular calcium levels. As increases of intracellular calcium are necessary for SHH signalling, we hypothesised that PLCH1 could be one of the mediators of the calcium intracellular signal generated by SHH binding to its receptors.[28] We speculate that PLCH1 has a role in the developmental responses to low levels of SHH, such as that generated by the spinal cord that then diffuses laterally to induce somite development. In holoprosencephaly, the SHH produced by the centrally placed caudal end of the notochord induces differentiation in the large prechordal plate, which grows caudally in all directions away from the notochord; hence, there will be a diminishing SHH gradient in outermost regions of the prechordal plate where we speculate PLCH1 to be expressed. Unfortunately, because of the unavailability of early human embryos (before Carnegie stage 10), we were unable to explore this. Taken together, our data suggest that PLCH1 could be a novel cause of autosomal recessive holoprosencephaly spectrum.

Author affiliations
[1]Cambridge Institute for Medical Research, University of Cambridge, Cambridge, UK
[2]Department of Genetics, King Faisal Specialist Hospital and Research Centre, Riyadh, Saudi Arabia
[3]Pediatrics, Prince Sultan Military Medical City, Riyadh, Al Riyadh, Saudi Arabia
[4]Human Developmental Biology Resource, Newcastle Institute of Genetic Medicine, Newcastle University, Newcastle, UK
[5]Especialista en Neurología Infantil, Hospital Universitario Quirónsalud de Madrid, Madrid, Spain
[6]Neuroradiology Section, Department of Radiology, Prince Sultan Military Medical, Riyadh, Saudi Arabia
[7]Department of Clinical Genetics, St Michaels Hospital Bristol, Bristol, UK
[8]Signalling Programm, Babraham Institute, Babraham Research Campus, Cambridge, UK
[9]Genetics, King Faisal Specialist Hospital and Research Center, Riyadh, Saudi Arabia
[10]Department of Anatomy and Cell Biology, College of Medicine, Alfaisal University, Riyadh, Saudi Arabia
[11]Cambridge Institute for Medical Research Cambridge, University of Cambridge, Cambridge, UK

Acknowledgements The authors thank the families for their participation in this research, Andreas Sagner and Professor James Briscoe of the Crick Institute for discussions on SHH function, and Professor Don Love for data on Young-Madder syndrome.

Contributors EF and ID conceived and performed experiments and were involved in writing the paper. RS, AF-J, SFS, KS, KT-G, FSA and GW produced clinical and experimental data. SLis and SLin produced the human embryo sections used in the paper, and were involved in the immunohistochemistry analysis. MN, HS, GW and FSA conceived and planned aspects of the project, and were involved in writing the paper.

Funding ID, EF and GW acknowledge funding by the 2017 Cambridge NIHR Cambridge Biomedical Research Centre award. MN by a Wellcome Trust Collaborative award (200183/Z/15/Z). A joint MRC/Wellcome Trust award (MR/R006237/1 and 099175/Z/12/Z) funds SLis and SLin. RS and FSA are supported by King Salman Centre for Disability Research and King Abdulaziz City for Science and Technology (13-BIO1113-20) and Saudi Human Genome Programme.

Competing interests None declared.

Patient consent for publication Parental/guardian consent obtained.

Ethics approval The consent of the family members to use their clinical information, or of parents if patients are children, was obtained according to the Declaration of Helsinki. The studies we performed have been approved by the Research Advisory Council (RAC) at King Faisal Specialist Hospital and Research Centre (RAC# 2121053) and Cambridge East Research Ethics Committee (05\Q0108\402).

Provenance and peer review Not commissioned; externally peer reviewed.

Data availability statement All data relevant to the study are included in the article or uploaded as supplementary information. GW's mail address: cw347@cam.ac.ukAddress: Cambridge Institute for Medical Research, University of Cambridge, Keith Peters Building, Addenbrookes Hospital, Hills Rd, Cambridge CB2 0QQ, UK.Website: https://www.cimr.cam.ac.uk/research/principal-investigators/woods.

ORCID iDs
Ichrak Drissi http://orcid.org/0000-0002-8077-2101
Steve Lisgo http://orcid.org/0000-0001-5186-3971
Alberto Fernández-Jaén http://orcid.org/0000-0003-3306-9832
Fowzan S Alkuraya http://orcid.org/0000-0003-4158-341X
Geoff Woods http://orcid.org/0000-0002-8077-2101

REFERENCES

1 Shiota K, Yamada S, Komada M, Ishibashi M. Embryogenesis of holoprosencephaly. *Am J Med Genet A* 2007;143A:3079–87.
2 Solomon BD, Gropman A, Muenke M. Holoprosencephaly Overview. In: Adam MP, Ardinger HH, Pagon RA, Wallace SE, Bean LJH, Stephens K, Amemiya A, eds. *GeneReviews® [Internet]*. Seattle (WA): University of Washington, 2000: 1993–2019.
3 Martinez AF, Kruszka PS, Muenke M. Extracephalic manifestations of nonchromosomal, nonsyndromic holoprosencephaly. *Am J Med Genet C Semin Med Genet* 2018;178:246–57.
4 Dubourg C, Bendavid C, Pasquier L, Henry C, Odent S, David V. Holoprosencephaly. *Orphanet J Rare Dis* 2007;2:1–14.
5 Taniguchi K, Anderson AE, Sutherland AE, Wotton D. Loss of Tgif function causes holoprosencephaly by disrupting the SHH signaling pathway. *PLoS Genet* 2012;8:e1002524.

6 Swatek J, Szumiło J, Burdan F. Alobar holoprosencephaly with cyclopia - autopsy-based observations from one medical center. *Reprod Toxicol* 2013;41:80–5.
7 Lewis AJ, Simon EM, Barkovich AJ, Clegg NJ, Delgado MR, Levey E, Hahn JS. Middle interhemispheric variant of holoprosencephaly: a distinct cliniconeuroradiologic subtype. *Neurology* 2002;59:1860–5.
8 Barkovich AJ, Guerrini R, Kuzniecky RI, Jackson GD, Dobyns WB. A developmental and genetic classification for malformations of cortical development: update 2012. *Brain* 2012;135:1348–69.
9 Solomon BD, Pineda-Alvarez DE, Gropman AL, Willis MJ, Hadley DW, Muenke M. High intellectual function in individuals with Mutation-Positive microform holoprosencephaly. *Mol Syndromol* 2012;3:201:140–2.
10 Solomon BD, Bear KA, Wyllie A, Keaton AA, Dubourg C, David V, Mercier S, Odent S, Hehr U, Paulussen A, Clegg NJ, Delgado MR, Bale SJ, Lacbawan F, Ardinger HH, Aylsworth AS, Bhengu NL, Braddock S, Brookhyser K, Burton B, Gaspar H, Grix A, Horovitz D, Kanetzke E, Kayserili H, Lev D, Nikkel SM, Norton M, Roberts R, Saal H, Schaefer GB, Schneider A, Smith EK, Sowry E, Spence MA, Shalev SA, Steiner CE, Thompson EM, Winder TL, Balog JZ, Hadley DW, Zhou N, Pineda-Alvarez DE, Roessler E, Muenke M. Genotypic and phenotypic analysis of 396 individuals with mutations in sonic hedgehog. *J Med Genet* 2012;49:473–9.
11 Nowaczyk MJM. Smith-lemli-opitz syndrome. In: Adam MP, Ardinger HH, Pagon RA, Wallace SE, eds. *GeneReviews® [Internet]*. Seattle (WA): University of Washington, 1998: 1993–2019.
12 Azurdia RM, Anstey AV, Rhodes LE. Cholesterol supplementation objectively reduces photosensitivity in the Smith-Lemli-Opitz syndrome. *Br J Dermatol* 2001;144:143–5.
13 Aoto K, Shikata Y, Higashiyama D, Shiota K, Motoyama J. Fetal ethanol exposure activates protein kinase A and impairs Shh expression in prechordal mesendoderm cells in the pathogenesis of holoprosencephaly. *Birth Defects Res A Clin Mol Teratol* 2008;82:224–31.
14 Roessler E, Hu P, Marino J, Hong S, Hart R, Berger S, Martinez A, Abe Y, Kruszka P, Thomas JW, Mullikin JC, Wang Y, Wong WSW, Niederhuber JE, Solomon BD, Richieri-Costa A, Ribeiro-Bicudo LA, Muenke M, NISC Comparative Sequencing Program. Common genetic causes of holoprosencephaly are limited to a small set of evolutionarily conserved driver genes of midline development coordinated by TGF-β, hedgehog, and FGF signaling. *Hum Mutat* 2018;39:1416–27.
15 Stouffer K, Nahorski M, Moreno P, Sarveswaran N, Menon D, Lee M, Geoffrey Woods C, Woods CG. Functional SNP allele discovery (fSNPd): an approach to find highly penetrant, environmental-triggered genotypes underlying complex human phenotypes. *BMC Genomics* 2017;18:944.
16 Bullen P, Wilson DI. The Carnegie staging of human embryos: a practical guide. In: Strachan T, Wilson DI, Lindsay S, eds. *Molecular genetics of early human development*. BIOS: Oxford, 1997: 27–50.
17 Young ID, Madders DJ. Unknown syndrome: holoprosencephaly, congenital heart defects, and polydactyly. *J Med Genet* 1987;24:714–5.
18 Mick DU, Rodrigues RB, Leib RD, Adams CM, Chien AS, Gygi SP, Nachury MV. Proteomics of primary cilia by proximity labeling. *Dev Cell* 2015;35:497–512.
19 Sheeba CJ, Andrade RP, Palmeirim I. Mechanisms of vertebrate embryo segmentation: common themes in trunk and limb development. *Semin Cell Dev Biol* 2016;49:125–34.
20 Kruszka P, Muenke M. Syndromes associated with holoprosencephaly. *Am J Med Genet C Semin Med Genet* 2018;178:229–37.
21 Bous SM, Solomon BD, Graul-Neumann L, Neitzel H, Hardisty EE, Muenke M. Holoprosencephaly-polydactyly/pseudotrisomy 13: a presentation of two new cases and a review of the literature. *Clin Dysmorphol* 2012;21:183–90.
22 Marquis-Nicholson R, Aftimos S, Ashton F, Love JM, Stone P, McFarlane J, George AM, Love DR. Pseudotrisomy 13 syndrome: use of homozygosity mapping to target candidate genes. *Gene* 2011;486:37–40.
23 Woods CG, Cox J, Springell K, Hampshire DJ, Mohamed MD, McKibbin M, Stern R, Raymond FL, Sandford R, Malik Sharif S, Karbani G, Ahmed M, Bond J, Clayton D, Inglehearn CF. Quantification of homozygosity in consanguineous individuals with autosomal recessive disease. *Am J Hum Genet* 2006;78:889–96.
24 Jobanputra V, Burke A, Kwame A-Y, Shanmugham A, Shirazi M, Brown S, Warburton PE, Levy B, Warburton D. Duplication of the ZIC2 gene is not associated with holoprosencephaly. *Am J Med Genet A* 2012;158A:103–8.
25 Stewart AJ, Morgan K, Farquharson C, Millar RP. Phospholipase C-eta enzymes as putative protein kinase C and Ca2+ signalling components in neuronal and neuroendocrine tissues. *Neuroendocrinology* 2007;86:243–8.
26 Miller JA, Ding S-L, Sunkin SM, Smith KA, Ng L, Szafer A, Ebbert A, Riley ZL, Royall JJ, Aiona K, Arnold JM, Bennet C, Bertagnolli D, Brouner K, Butler S, Caldejon S, Carey A, Cuhaciyan C, Dalley RA, Dee N, Dolbeare TA, Facer BAC, Feng D, Fliss TP, Gee G, Goldy J, Gourley L, Gregor BW, Gu G, Howard RE, Jochim JM, Kuan CL, Lau C, Lee C-K, Lee F, Lemon TA, Lesnar P, McMurray B, Mastan N, Mosqueda N, Naluai-Cecchini T, Ngo N-K, Nyhus J, Oldre A, Olson E, Parente J, Parker PD, Parry SE, Stevens A, Pletikos M, Reding M, Roll K, Sandman D, Sarreal M, Shapouri S, Shapovalova NV, Shen EH, Sjoquist N, Slaughterbeck CR, Smith M, Sodt AJ, Williams D, Zöllei L, Fischl B, Gerstein MB, Geschwind DH, Glass IA, Hawrylycz MJ, Hevner RF, Huang H, Jones AR, Knowles JA, Levitt P, Phillips JW, Sestan N, Wohnoutka P, Dang C, Bernard A, Hohmann JG, Lein ES. Transcriptional landscape of the prenatal human brain. *Nature* 2014;508:199–206.
27 Hwang J-I, Oh Y-S, Shin K-J, Kim H, Ryu SH, Suh P-G. Molecular cloning and characterization of a novel phospholipase C, PLC-eta. *Biochem J* 2005;389:181–6.
28 Klatt Shaw D, Gunther D, Jurynec MJ, Chagovetz AA, Ritchie E, Grunwald DJ. Intracellular calcium mobilization is required for sonic hedgehog signaling. *Dev Cell* 2018;45:512–25.

Supplementary Table

Title: Exome filtering scheme and the list of survived and potential pathogenic variants found in Family one and Family two.

	Family One	**Family Two**
Filtering Scheme		
Total number of variants	38019	166318 + 171659
Homozygous variants	15731	94128 + 100282
Coding/splicing	9991	3596 + 3516
Family One: 1000 genomes MAF <0.001	621	na
Family Two: concordance	na	26
Within the autozygome	22	23
Family One: Human Saudi Genome Project database: frequency <0.01 **Family Two: gnomAD frequency <0.001**	1. *PLCH1*:NM_001130960.1:c.2109T>C, p.(=) (synonymous SNV) 2. *PLCH1*:NM_001130960.1: c.2065C>T: p.(Arg689*) (stopgain) 3. *SMC4*:NM_005496:c.2673C>A:p.I891I (synonymous SNV) 4. *C20orf141*:NM_080739: c.265G>A:p.A89T (nonsynonymous SNV) 5. *PCNA*: NM_002592:c.388-18A>C	1. *PLCH1*:NM_001130960.1: c.3236CA>C: p.(Cys1079ValfsTer16) (frameshift)
Predicted to be pathogenic	1. *PLCH1*:NM_001130960.1: c.2065C>T: p.(Arg689*) (stopgain)	1. *PLCH1*:NM_001130960.1: c.3236CA>C: p.(Cys1079ValfsTer16) (frameshift)

SUPPLEMENTARY MATERIAL

Clinical data

In Family one, the first ascertained case was a five year old boy, born at 41weeks gestation by Caesarean section due to difficult labour because of large head size. His birth weight was 3.39 kg (25-50th centile), length was 51 cm, and OFC was 39 cm (>99.6th centile). Positive findings on examination included frontal bossing, upturned nose, large ears and generalized hypotonia. Postnatal brain MRI revealed partial agenesis of the corpus callosum, a well-defined cystic lesion within the left lateral ventricle near the foramen of Monro, see Figure 1. The lesion had a similar signal intensity to the white matter on T1 but displayed bright signal intensity on T2, findings consistent with subependymal cyst. Although ventriculomegaly was apparent, there was no evidence of CSF permeation to suggest active hydrocephalus. In addition, there was right periventricular heterotopia and enlarged cisterna magna. Follow up revealed persistence macrocephaly and a repeat MRI at age nine months showed evolving leukomalacia in both cerebral hemispheres more on the left with diffuse ventriculomegaly sparing the fourth ventricle. Sagittal T2 was suggestive of aqueduct stenosis. He underwent endoscopic third ventriculostomy with fenestration of pineal cyst. However, he developed tonic clonic epilepsy one month postoperatively with only partial response to dual therapy with carbamizapine and keppra. His development was grossly delayed: he only walked at age four years and age five years his vocabulary is limited to 10 words. His most recent growth parameters at five years of age are OFC 54 cm, height 114 cm, and weight 34 kg. Parents are Sudanese first cousins with three normal children and one deceased similarly affected daughter.

In Family one available records on the affected sister revealed that she was born with multiple congenital anomalies in the form of Dandy-Walker malformation, hydrocephalus necessitating a ventriculo-peritoneal shunt placement, ventricular septal defect, cleft lip and palate (Bilateral cleft lip and palate) and epilepsy with abnormal EEG (persistent spikes) started at age of 10 days. Brain MRI revealed a large posterior fossa cyst with atrophy of the cerebellum and partial agenesis of the vermis, suggestive of Dandy Walker Malformation. It also revealed heterotopia in both cerebral hemispheres, posteriorly kinked midbrain, atrophic pons, and a large interhemispheric cyst communicating with the third and lateral ventricles. A follow up MRI showed evidence of an enlarged and disfigured ventricular system, giving the appearance of a monoventricle with absent septum pellucidum, findings suggestive of holoprosencephaly, see Figure 1. The ventricular system appeared to be

separated from a dorsal cyst by thin layers. She passed away because of multiple complications of her surgery and no DNA was available.

In Family two, the first affected was a male infant. At 20 weeks of gestation, he was noted on antenatal ultrasound to have holoprosencephaly. Further ultrasound scanning confirmed alobar holoprosencephaly, midline cleft lip, microcephaly and cardiac abnormality (double outlet right ventricle, ventricular septal defect and possible aortic atresia). He was born at term but died shortly after birth. He also had cyclopia. The parents declined post-mortem examination. He had a normal male karyotype and no evidence of 22q11 deletion.

In Family two the next pregnancy was an affected female infant. Early antenatal ultrasound scans showed probable holoprosencephaly, with the cranium being almost entirely fluid filled and only brain stem structures present. No other abnormalities were reported. She died a few hours after birth. Facial features included ears completely low set and joining together under the chin area and no eyes as such but disrupted tissue beneath a proboscis. The parents declined post-mortem examination. The baby had a normal female karyotype.

The parents are British-Pakistani first cousins. Their first baby was a male infant born at 33 weeks. He had an intra-cranial haemorrhage at age 24 days attributed to haemorrhagic disease of the new-born. There was no underlying structural brain abnormality. This appeared to cause secondary hydrocephalus and cerebral atrophy. He had severe developmental delay and epilepsy. He was subsequently diagnosed with extra hepatic biliary atresia and died aged two years from a chest infection shortly after gastrostomy operation. No DNA was available and chromosome analysis had not been performed. The couple then had an intrauterine death at 17 weeks gestation, and then a healthy son.

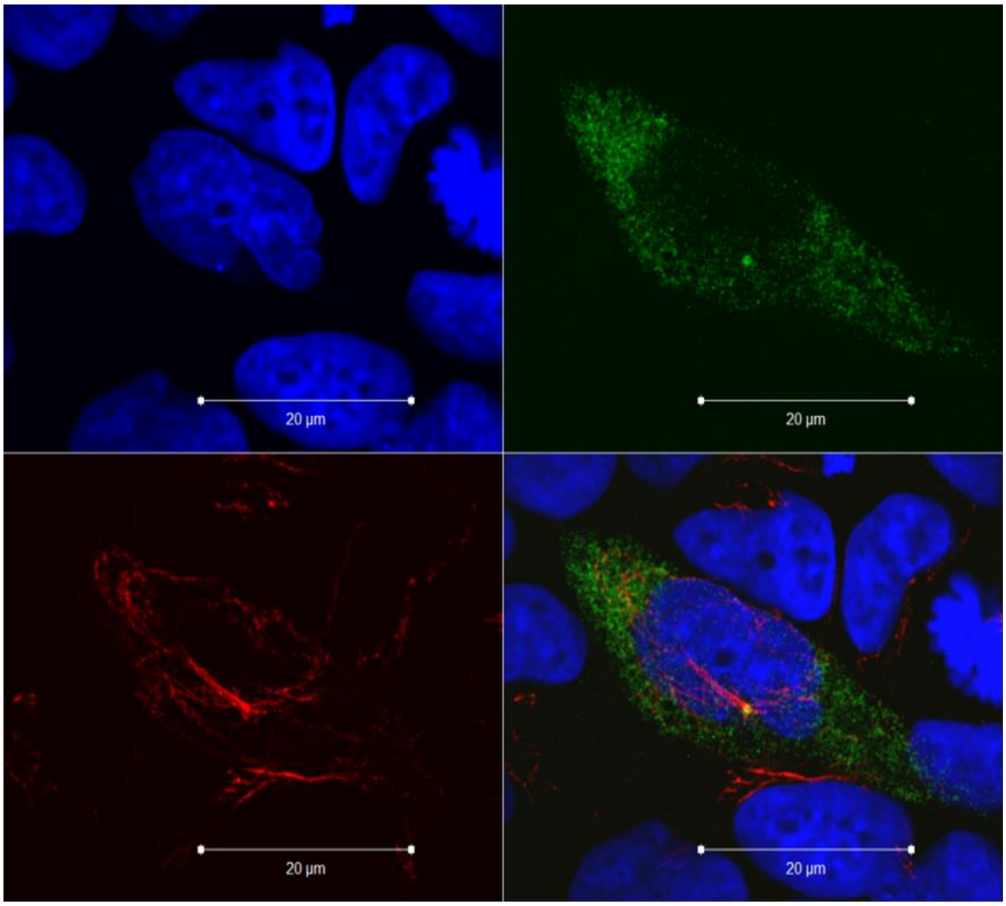

Title: Assessment of the subcellular localisation of PLCH1, with the primary cilium identified.

Legend: Confocal Microscopy images of immunofluorescent studies of the localisation of wild-type PLCH1 (green) in 1-7 HB2 cells with primary cilia identified by (red). PLCH1 is distributed throughout the cytoplasm of the cell. PLCH1 was not being present in the primary cilium or nucleus. Green shows FLAG-tagged PLCH1, red shows acetylated α-tubulin as a primary cilia marker, and the nucleus identified in blue by DAPI.

Supplementary Table

Title: Exome filtering scheme and the list of survived and potential pathogenic variants found in Family one and Family two.

	Family One	**Family Two**
Filtering Scheme		
Total number of variants	38019	166318 + 171659
Homozygous variants	15731	94128 + 100282
Coding/splicing	9991	3596 + 3516
Family One: 1000 genomes MAF <0.001	621	na
Family Two: concordance	na	26
Within the autozygome	22	23
Family One: Human Saudi Genome Project database: frequency <0.01 **Family Two: gnomAD frequency <0.001**	1. *PLCH1*:NM_001130960.1:c.2109T>C, p.(=) (synonymous SNV) 2. *PLCH1*:NM_001130960.1: c.2065C>T: p.(Arg689*) (stopgain) 3. *SMC4*:NM_005496:c.2673C>A:p.I891I (synonymous SNV) 4. *C20orf141*:NM_080739: c.265G>A:p.A89T (nonsynonymous SNV) 5. *PCNA*: NM_002592:c.388-18A>C	1. *PLCH1*:NM_001130960.1: c.3236CA>C: p.(Cys1079ValfsTer16) (frameshift)
Predicted to be pathogenic	1. *PLCH1*:NM_001130960.1: c.2065C>T: p.(Arg689*) (stopgain)	1. *PLCH1*:NM_001130960.1: c.3236CA>C: p.(Cys1079ValfsTer16) (frameshift)

SUPPLEMENTARY MATERIAL

Clinical data

In Family one, the first ascertained case was a five year old boy, born at 41weeks gestation by Caesarean section due to difficult labour because of large head size. His birth weight was 3.39 kg (25-50th centile), length was 51 cm, and OFC was 39 cm (>99.6th centile). Positive findings on examination included frontal bossing, upturned nose, large ears and generalized hypotonia. Postnatal brain MRI revealed partial agenesis of the corpus callosum, a well-defined cystic lesion within the left lateral ventricle near the foramen of Monro, see Figure 1. The lesion had a similar signal intensity to the white matter on T1 but displayed bright signal intensity on T2, findings consistent with subependymal cyst. Although ventriculomegaly was apparent, there was no evidence of CSF permeation to suggest active hydrocephalus. In addition, there was right periventricular heterotopia and enlarged cisterna magna. Follow up revealed persistence macrocephaly and a repeat MRI at age nine months showed evolving leukomalacia in both cerebral hemispheres more on the left with diffuse ventriculomegaly sparing the fourth ventricle. Sagittal T2 was suggestive of aqueduct stenosis. He underwent endoscopic third ventriculostomy with fenestration of pineal cyst. However, he developed tonic clonic epilepsy one month postoperatively with only partial response to dual therapy with carbamizapine and keppra. His development was grossly delayed: he only walked at age four years and age five years his vocabulary is limited to 10 words. His most recent growth parameters at five years of age are OFC 54 cm, height 114 cm, and weight 34 kg. Parents are Sudanese first cousins with three normal children and one deceased similarly affected daughter.

In Family one available records on the affected sister revealed that she was born with multiple congenital anomalies in the form of Dandy-Walker malformation, hydrocephalus necessitating a ventriculo-peritoneal shunt placement, ventricular septal defect, cleft lip and palate (Bilateral cleft lip and palate) and epilepsy with abnormal EEG (persistent spikes) started at age of 10 days. Brain MRI revealed a large posterior fossa cyst with atrophy of the cerebellum and partial agenesis of the vermis, suggestive of Dandy Walker Malformation. It also revealed heterotopia in both cerebral hemispheres, posteriorly kinked midbrain, atrophic pons, and a large interhemispheric cyst communicating with the third and lateral ventricles. A follow up MRI showed evidence of an enlarged and disfigured ventricular system, giving the appearance of a monoventricle with absent septum pellucidum, findings suggestive of holoprosencephaly, see Figure 1. The ventricular system appeared to be

separated from a dorsal cyst by thin layers. She passed away because of multiple complications of her surgery and no DNA was available.

In Family two, the first affected was a male infant. At 20 weeks of gestation, he was noted on antenatal ultrasound to have holoprosencephaly. Further ultrasound scanning confirmed alobar holoprosencephaly, midline cleft lip, microcephaly and cardiac abnormality (double outlet right ventricle, ventricular septal defect and possible aortic atresia). He was born at term but died shortly after birth. He also had cyclopia. The parents declined post-mortem examination. He had a normal male karyotype and no evidence of 22q11 deletion.

In Family two the next pregnancy was an affected female infant. Early antenatal ultrasound scans showed probable holoprosencephaly, with the cranium being almost entirely fluid filled and only brain stem structures present. No other abnormalities were reported. She died a few hours after birth. Facial features included ears completely low set and joining together under the chin area and no eyes as such but disrupted tissue beneath a proboscis. The parents declined post-mortem examination. The baby had a normal female karyotype.

The parents are British-Pakistani first cousins. Their first baby was a male infant born at 33 weeks. He had an intra-cranial haemorrhage at age 24 days attributed to haemorrhagic disease of the new-born. There was no underlying structural brain abnormality. This appeared to cause secondary hydrocephalus and cerebral atrophy. He had severe developmental delay and epilepsy. He was subsequently diagnosed with extra hepatic biliary atresia and died aged two years from a chest infection shortly after gastrostomy operation. No DNA was available and chromosome analysis had not been performed. The couple then had an intrauterine death at 17 weeks gestation, and then a healthy son.

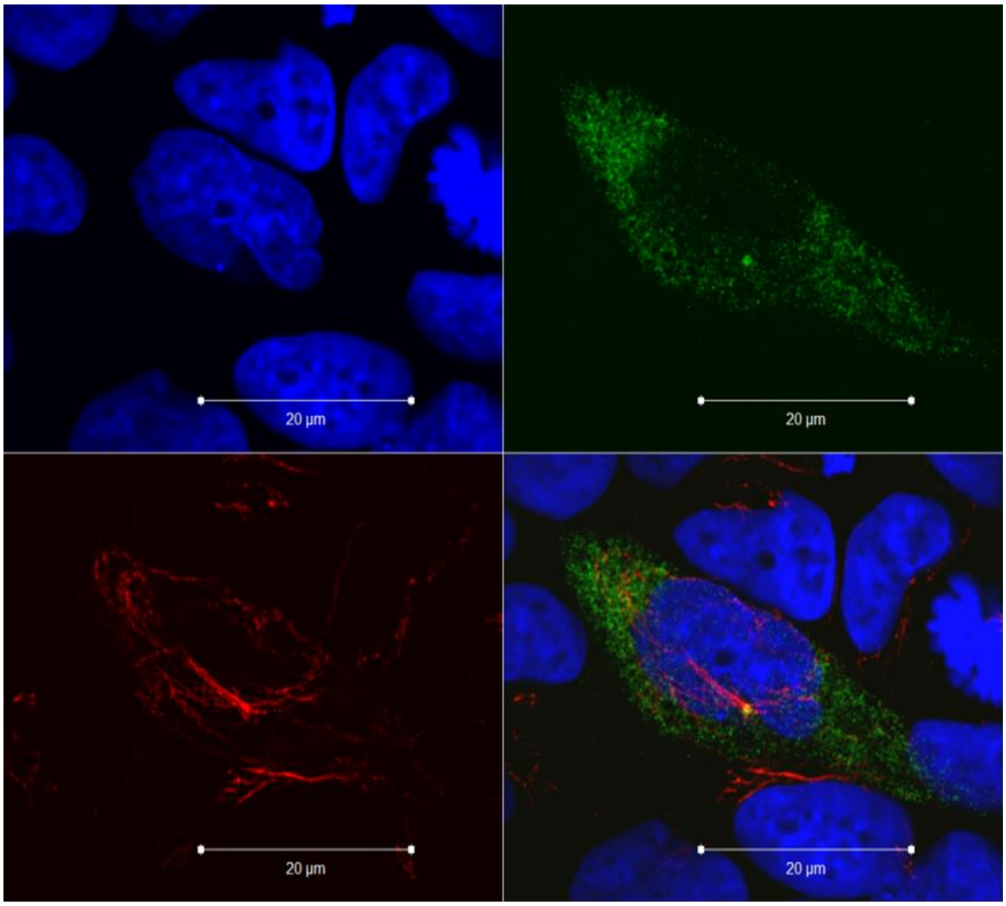

Title: Assessment of the subcellular localisation of PLCH1, with the primary cilium identified.

Legend: Confocal Microscopy images of immunofluorescent studies of the localisation of wild-type PLCH1 (green) in 1-7 HB2 cells with primary cilia identified by (red). PLCH1 is distributed throughout the cytoplasm of the cell. PLCH1 was not being present in the primary cilium or nucleus. Green shows FLAG-tagged PLCH1, red shows acetylated α-tubulin as a primary cilia marker, and the nucleus identified in blue by DAPI.